MRI characterization of a focal rat brain necrosis induced by interlaced microbeam radiation therapy.

R. Serduc[1,2], N. Pannetier[3], A. Bouchet[2], T. Brochard[2], T. Christen[3], G. Berruyer[4], J. Laissue[5], F. Esteve[3], C. Remy[3], E. Barbier[3], A. Bravin[2], G. Le Duc[2], and E. Brauer[2]

[1]CERCO, CNRS, Toulouse, France, [2]Imaging Group, ESRF, Grenoble, France, [3]U836, INSERM, Grenoble, France, [4]Scisoft Group, ESRF, Grenoble, France, [5]Bern Institute of pathology, Bern, Switzerland

Introduction

Microbeam Radiation Therapy (MRT) is a preclinical form of radiosurgery which has been first dedicated to brain tumor treatment. It uses micrometer-wide synchrotron-generated X-ray beams and is based on the principle of spatial beam fractionation instead of clinically-used temporal fractionation (1, 2). The normal brain of different animal species showed a surprising resistance to very high radiation doses (hundreds of Gy) applied in the MRT mode (3, 4). The exceptional radioresistance of normal brain vasculature to MRT allows a continuous blood supply, thus preventing brain necrosis which may occur after conventional radiotherapy. (5, 6). On the basis of this well characterized normal tissue sparing effect of irradiations in the MRT mode, we now have developed a new method which allows a uniform deposition of a high dose in the radiation target. We have characterized the evolution of the ensuing brain lesion using MRI and immunohistology.

Methods

Normal rat brains (n=24) were exposed to 4 interlaced arrays of 10 microbeams (52µm wide, spaced 200µm on-center, 50 to 350keV in energy, see figure 1a) with an in microbeam-dose at 1cm depth of 175Gy, resulting in a 200Gy dose focused and homogeneously delivered in a volume of 2.2x2x2mm^3 in the caudate nucleus of rat brains. Three to eight rat brains were imaged on a 7T Bruker system at different delays after exposure *i.e.* 1, 4, 7, 15, 30, 60 and 90 days. Radiation-induced anatomical changes were checked on T_2-weighted images (Turbo RARE Seq. TR: 5s, TE: 33ms). The apparent diffusion coefficient (ADC) was mapped using a diffusion tensor MR sequence (b=0 and b=1000 s.mm^{-2}). Brain vessel permeability was then characterized using a T_1-weighted MR sequence (Turbo RARE Seq. TR: 950ms TE: 7.7ms) acquired 5 min after Gd-DOTA i.v. injection (200µmol.kg^{-1}). Two regions of interest were defined: the radiation target in right caudate and the contralateral left caudate nucleus. A two way ANOVA test (Bonferroni posttest) was used to compare different data groups (*: $p<0.05$, **: $p<0.01$, ***: $p<0.001$). Four rats were randomly sacrificed for histological studies at 1, 7, 15, 30 and 60 days after irradiation. Immunohistochemistry for gamma-H2AX (radiation-induced DNA damages), Ki67 (mitosis index), ED1 (macrophage labeling), GFAP (astrocytes) NeuN (neurons) and Type IV collagen (brain vessels) were performed on 20µm thick frozen brain sections. Three rats were kept alive to be imaged at a longer delay after exposure (6 months) to characterize the late effects of interlaced MRT on normal brain.

Results and discussion

MRI follow-up of rats showed a gradual increase of T_1w signal values after Gd-DOTA injection in the irradiation target starting at day 7 and which became significant at 15 days after exposure (fig 2). Three rats out of 7, 8/8, and 8/8 (at days 7, 15 and 30 days after irradiation respectively) showed a highly localized extravation of Gd-DOTA, confined to the radiation target (Fig 1b-1c). There was no significant difference in T_1w signal values at longer delays after MRT exposure; only isolated and dotted signal of Gd-DOTA situated in the irradiation target were observed on T_1w images. This transient T_1w values modification reflects an increase in blood vessel permeability within the radiation target. This observation was in good agreement with our histological analysis which revealed that only the interlaced region exhibited a quasi-uniform labeling of damaged DNA 24h after irradiation (fig. 1e, compared with the spatially fractionated microbeam irradiation in the contralateral hemisphere fig 1d). The same labeling pattern was observed for astrocytes and macrophages. Rarefaction of blood vessels (fig 1g, contralateral hemisphere fig 1f), most likely due to necrosis, and an increase in the diameter of remaining vessels were prominent one month after irradiation. Simultaneously, a brain edema was detected by a significant increase in ADC and T_2w signal values (fig 2), and a localized hypersignal on T_2 images. T_1w and T_2w signal decreased to normal values at day 60 and 90 while the ADC remained significantly higher in the irradiation target compared with the contralateral caudate. These high ADC values reflect tissular changes induced by high radiation doses in the target. Histological signs of necrosis were observed 30 days after radiation exposure on brain sections stained with hematoxylin and eosin (data not shown).

Conclusions

Interlaced MRT allowed a high dose deposition in rat brain and induced uniform tissue changes compatible with necrosis while sparing surrounding tissues. Our recent Monte-Carlo simulations (7) revealed that synchrotron-generated x-rays, despite their low energy, are a promising tool for high uniform dose delivery in human brains with the sharpest dose fall-off ever described in radiotherapy (8). This irradiation modality could be used to treat all of the brain lesions amenable to radiosurgery *i.e.,* tumors, arteriovenous malformations, pharmaco-resistant epilepsy and other circumscribed lesions. They may allow the treatment of lesions that are not surgically resectable, with minimal normal tissue damage. MRI would be useful to follow the efficacy of such treatments and interlaced MRT treatments of 9L gliosarcoma implanted in rat brains are now foreseen.

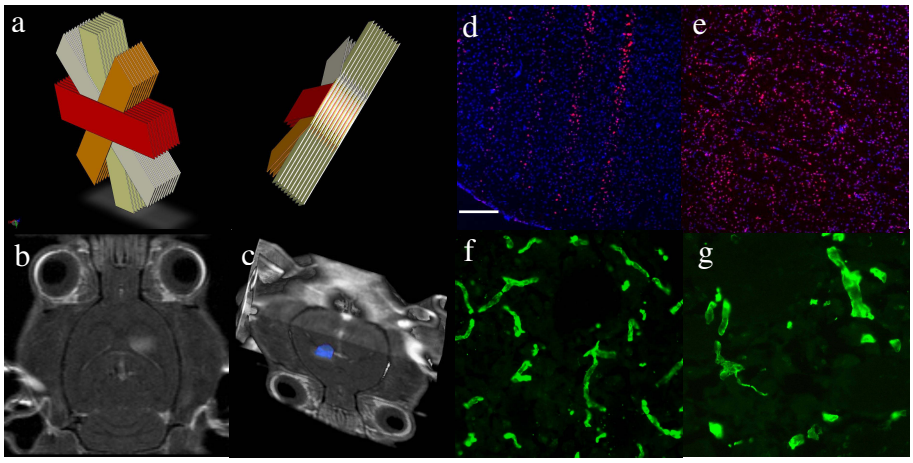

Fig 1: a- Irradiation geometry used for interlaced microbeam radiation therapy. b- T_1-w MR-image after Gd-DOTA i.v. injection, 30 days after irradiation. c- 3D image reconstruction of the irradiated target (blue) based on Gd-DOTA extravasation on T_1-weighted images. Radiation-induced DNA damages in the contralateral cortex (d) and in the radiation target (e) 24h after exposure (p-H2AX immunochemistry). Brain vessel immunolabeling (Type IV collagen) in the contralateral caudate (f) and in the irradiation target (g) 1 month after irradiation. Scale bar represents 200 and 50 µm in d/e and f/g respectively.

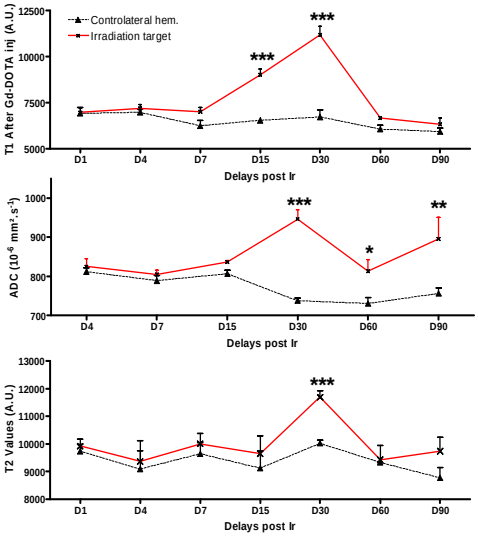

Fig 2: T_1w signal values, ADC and T_2 signal values measured in the irradiated target and in the contralateral caudate at different delays after radiation exposure.

References : 1.Slatkin, D. N. *et al.,* (1994), United States patent. 2.Slatkin, D. N. *et al.,* (1992) *Med Phys* **19,** 1395-400. 3.Regnard, P. *et al.,* (2008) *Phys Med Biol* **53,** 861-78. 4.Laissue, J. A. *et al., Dev Med Child Neurol* **49,** 577-81. 5.Serduc, R. *et al.,* (2008) *Phys Med Biol* **53,** 1153-66. 6.Serduc, R. *et al.,* (2006) *Int J Radiat Oncol Biol Phys* **64,** 1519-27. 7.Siegbahn, E., A. *et al.,* & (2006) *Med. Phys.* **33,** 3248-59. 8.Dilmanian, F. A., *et al.,* (2006) *Proc Natl Acad Sci U S A* **103,** 9709-14.